

Automated Surface Texture Classification of Inkjet and Photographic Media

Paul Messier; Paul Messier LLC, Boston, MA USA; Richard Johnson; Cornell University, Ithaca, NY USA; Henry Wilhelm; Wilhelm Imaging Research, Inc., Grinnell, Iowa USA; William A. Sethares; University of Wisconsin, Madison, WI, USA; Andrew G. Klein; Worcester Polytechnic Institute, Worcester, MA USA; Patrice Abry; Ecole Normale Supérieure de Lyon, Centre National de la Recherche Scientifique, Lyon FR; Stéphane Jaffard; University of Paris, Paris FR; Herwig Wendt, Institute de Recherche en Informatique de Toulouse, Centre National de la Recherche Scientifique; Toulouse, FR; Stéphane Roux, Ecole Normale Supérieure de Lyon, Lyon FR; Nelly Pustelnik, Ecole Normale Supérieure de Lyon, Centre National de la Recherche Scientifique, Lyon FR; Nanne van Noord, Laurens van der Maaten, and Eric Postma; Tilburg University, Tilburg, NL

Abstract

Digital imaging and signal processing technologies offer new methods for inkjet and photographic media engineers and manufacturers, and those responsible for product quality control, to classify and characterize printing materials surface textures using new and more quantitative methods. This paper presents a collaborative project to systematically and semi-automatically characterize the surface texture of inkjet media. These methods have applications in product design and specification, and in manufacturing quality control.

Surface texture is a critical feature in the manufacture, marketing and use of inkjet papers, especially those used for fine art printing. Raking light reveals texture through a stark rendering of highlights and shadows. Though raking light photomicrographs effectively document surface features of inkjet paper, the sheer number and diversity of textures prohibits efficient visual classification. This work provides evidence that automatic, computer-based classification of texture documented with raking light photomicrographs is feasible by demonstrating an encouraging degree of success sorting a set of 120 photomicrographs made from diverse samples of inkjet paper and canvas available in the market from 2000 through 2011.

The samples used for this study were drawn from the *Wilhelm Analog and Digital Color Print Materials Reference Collection*. Using this dataset, four university teams applied differ-

ent image processing strategies for automatic feature extraction and degree of similarity quantification. All four approaches were successful in detecting strong affinities among similarity groupings built into the dataset as well as identifying outliers. The creation and deployment of the algorithms was carried out by the teams without prior knowledge of the distributions of similarities and outliers. These results indicate that automatic classification of inkjet paper based on texture photomicrographs is feasible. To encourage the development of additional classification schemes, the 120 inkjet sample “training” dataset used in this work is available to other academic researchers at www.PaperTextureID.org.

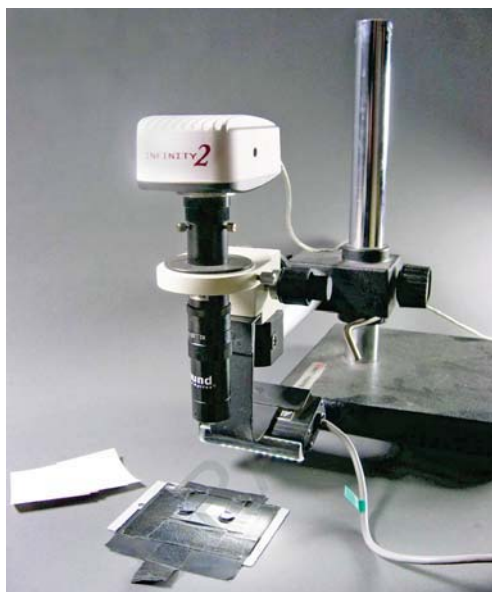


Figure 1. Microscope and light configuration for producing raking light photomicrographs.

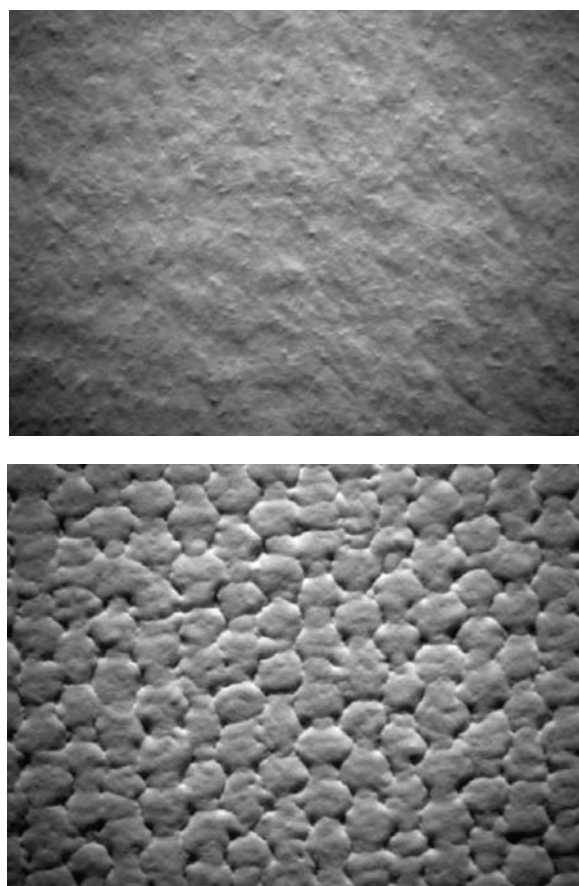


Figure 2. Raking light photomicrographs: Hahnemühle Fine Art William Turner: Germany, ~2009 (top) and Canson Museum Canvas Water Resistant Matte Canvas: France, April 2008 (bottom).

Texture in Inkjet and Photographic Media

Texture is a defining attribute of traditional photographic paper. Starting in the early 20th century, manufacturers manipulated texture to differentiate their papers and to satisfy the aesthetic and functional requirements of photographers. Especially prior to WWII, when black and white silver gelatin paper was the dominant photographic medium, dozens of manufacturers worldwide produced a wide array of surfaces.[1] Surfaces were proprietary to the different manufacturers and each was used across their multiple brands of paper with changes, additions, and deletions occurring over a span of many years. Inkjet papers, especially those geared for the art market, show an even greater differentiation and diversity of surface texture.

A vital factor in the evaluation of paper surface, texture impacts the visibility of fine detail and thus provides insight into the intent of the photographer and the envisioned purpose of a particular print. For example, prints made for reproduction or documentary functions tend to be better suited to smooth-surface papers that render details with sharpness and clarity whereas more impressionistic or expressive subjects, especially those depicting large unmodulated masses of shadows or highlights, are best suited for papers with rough, broadly open textures.[2]

A result of a careful and deliberate manufacturing process, texture applied to inkjet paper is designed to be distinct and distinguishable by artists and discerning viewers. Given these attributes, an encyclopedic collection of surface textures could have forensic or art historical research value providing vital clues about a questioned print of unknown origin.

Previous work established the use of photomicrographs as a simple and effective means to gather texture data.[3-4] Further, recent research into historic silver gelatin papers showed a high level of success sorting texture photomicrographs using algorithms developed independently by four university teams.[5] By applying these algorithms to inkjet papers, this work is based directly on the previous research into silver gelatin surfaces and provides a useful basis for comparing results.

Texture Image Preparation

Sample inkjet papers and canvas dating from 2000 to 2011 were selected from the *Wilhelm Analog and Digital Color Print Materials Reference Collection*, which includes a large number of inkjet papers and canvas.[6] To the extent possible, each sample was identified by manufacturer, brand, date, and manufacturer-assigned surface designation.

The texture images were acquired with a microscope system assembled using an Infinity 2-3 imager manufactured by the Lumenera Corporation fitted with an Edmund Optics VZM 200i lens, as shown in Figure 1.

The imager incorporates an Interline Sony ICX262 3.3 megapixel color progressive scan CCD sensor producing images that incorporate 1536 x 2080, 3.45 μ m, square pixels. The imaged area on each sample measured 1.00 x 1.35 cm. Raking light photomicrographs were made using a fixed point illumination source with a 3-inch LED line light manufactured by Advanced Illumination placed at a 25° raking angle to the surface of the photographic paper.

Each raking light photomicrograph generated a 16-bit TIFF. Typical samples are shown in Figure 2. The image capture technique is non-contact / non-destructive and therefore easily adapted for use on prints of high intrinsic value.

Collaborative Competition

As part of a materials-based characterization project of modernist silver gelatin photographs at the Museum of Modern Art (MoMA) in New York, raking light photomicrographs were made from each print from the Thomas Walther Collection to document surface texture. This work stimulated interest in developing an automated scheme to cluster like prints based on surface texture. An appeal was made to university teams with signal processing experience to initiate a collaborative competition to develop methods for sorting texture images.

Four university teams joined this project:

University of Wisconsin: William A. Sethares

Worcester Polytechnic Institute: Andrew G. Klein,

Christopher Brown, Anh Hoang Do, and Philip Klausmeyer

Ecole Normale Supérieure de Lyon: Patrice Abry, Stéphane Jaffard, Herwig Wendt Stéphane Roux, and Nelly Pustelnik

Tilburg University: Nanne van Noord, Laurens van der Maaten, and Eric Postma

Each team adopted a different approach to the development of the two standard parts of an automatic classifier: (1) feature vector extraction and (2) degree of similarity quantification. These strategies stem from a broad variety of basic approaches to texture image classification and are described in the following section.[7]

Prototype algorithms were constructed by the four teams using a training set of 50 silver gelatin samples with some known texture matches. This preliminary work established that the orientation of the primary paper fiber direction relative to the raking light had no significant impact on results. This finding does not exclude *a priori* that silver gelatin surfaces possess other forms of anisotropy. This initial work proved effective in providing a basis for sorting silver gelatin prints by surface texture. Since inkjet surfaces were not included in this preliminary test and some surfaces appear to exhibit anisotropy based on fiber direction, a natural expansion of the scope of this work, immediate interest was expressed in testing the applicability of the data collection method and sorting strategies on other paper surfaces including inkjet paper and canvas.

To forward these goals, a dataset containing 120 raking light photomicrographs of inkjet papers with known metadata including manufacturer, brand, date, gloss, and texture classification, and offering varying degrees of self-similarity was prepared (the Appendix lists all samples used in this study). The dataset delivered to the teams for testing was largely composed of nine groups of ten paper samples each. Within these groups, there were three similarity subsets: (1) images made from the same sheet of paper, (2) images made from sheets taken from the same manufacturer package of paper and, (3) images from papers made to the same manufacturer specifications over a period of time. The remaining thirty samples were picked without concern for texture similarity but instead were selected to span the large range of textures associated with inkjet paper.

Conventional wisdom suggests that any raking light photomicrograph taken from different spots on a single sheet of paper would appear nearly identical. Likewise, texture images from different sheets of paper taken from the same manufacturer package also should show strong similarity. Furthermore, raking light images from papers manufactured to the same specifications but made at different times should show strong similarity, but to a somewhat lesser degree. For the thirty remaining samples, selected to demonstrate diversity, some would appear similar to the group of ninety textures and some would appear to be unique. The challenge posed to the teams was to discover these similarity groupings and isolate unique textures by producing a system of texture affinities that described the entire set.

Technical Approaches

The approaches taken by the four teams can be divided into two categories [8] based on the approach to feature definition: (1) non-semantic / Wisconsin and Tilburg and (2) multiscale / Lyon and WPI. The fundamental difference is that non-semantic features are derived directly from the image data where multiscale features are based on a structural model presupposed as relevant to the encountered data.

1. Eigentextures (Wisconsin)

In the eigentexture approach, a collection of small patches are chosen from each photographic image. These patches are gathered into a large matrix and then simplified to retain only the most relevant eigendirections using a singular value decomposition (SVD).[9] The preparation stage consists of two steps:

1. For each imaged paper j , randomly pick N $p \times p$ pixel patches $X_{j,i} \in \mathbb{R}^{p \times p}$ for $i = 1, 2, \dots, N$ (with $N = 2000$ and $p = 25$ in this case). Lexicographically reorder the $X_{j,i}$ into column vectors $a_{j,i} \in \mathbb{R}^{p^2}$.
2. Create matrices $A_j = [a_{j,1} \ a_{j,2} \ \dots \ a_{j,N}]$ consisting of the N column vectors and calculate the SVDs $A_j = U_j \Sigma V_j^T$ for all j . Extract the m columns of U_j corresponding to the m largest singular values and call this U_j (with m selected as 15 in this case).

The U_j are the representatives of the classes and may be thought of as vectors pointing in the most-relevant directions. During the classification stage, a number of similarly-sized patches are drawn from the tested photographic paper. Each of these patches is compared to the representatives of the classes via a least squares (LS) procedure.

3. Select Q (with $Q = 2000$ used here) $p \times p$ pixel patches Q_i from the tested paper and reorder into vectors $q_i \in \mathbb{R}^{p^2}$. Calculate the distance from the i th patch to the j th class:

$$d(i, j) = \left\| q_i - U_j (U_j^T q_i) \right\|_2. \quad (1)$$

Every patch is closest to one of the classes, and the number of patches closest to the j th class is recorded.

4. For each patch i , $f_i = \text{argmin}_j d(i, j)$ locates the smallest of the $d(i, j)$, indicating that class j is the best fit for patch i . Tally the set of all such f_i , $i = 1, 2, \dots, Q$.

The commonest entry among the f_i is the most likely class for this image. The second most common entry is the next most likely class for this image, etc.

2. Random-feature texton method (Tilburg)

This method combines random features and textons, i.e., the random-feature texton method. This method was developed by Liu and Fieguth [10] and is an adaptation of the texton approach [11] using random features. Textons are prototypical exemplar image patches capturing the ‘‘essence’’ of the texture of an image. Random-features (RF) are random projections of image patches with $N \times N$ pixels to vectors with D elements ($N = 9$, $D = 20$, $D < N \times N$). More specifically, a random feature (RF) is defined as a $D \times N^2$ matrix, the elements of which are sampled from the standard multivariate normal distribution $\mathcal{N}(0,1)$.

The application of the random-feature texton method on the 120-sample dataset is conducted as follows. A set of X sub-images of $M \times M$ pixels is selected for each gray-value texture image in the 120 sample dataset ($M = 512$). The sub-images are defined to be the central regions of $M \times M$ pixels of which the intensity distributions are normalized to zero mean and unit variance. A sample of 45,000 randomly selected $N \times N$ ($N \ll M$) patches (represented as vectors of length N^2) of the normalised sub-images are contrast-normalised and subsequently multiplied with RFs, yielding RF vectors of length D .

Subsequently, a texton dictionary is created by applying k-means clustering to all RF vectors of the X sub-images of each texture image of the 120-sample dataset. Each image of the dataset is transformed into a texture histogram by comparing all of its patches (represented as RF vectors) to the entries in the texton dictionary. Finally, the histograms are classified using a k-nearest neighbor algorithm using the χ^2 similarity measure.

3. Anisotropic wavelet multiscale analysis (Lyon)

This method relies on the use of the Hyperbolic Wavelet Transform (HWT) [12–13] which is a variation of the 2D-Discrete Wavelet Transform (2D-DWT).[14] The HWT explicitly takes into account the possible anisotropic nature of image textures. Indeed, instead of relying on a single dilation factor a used along both directions of the image (as is the case for the 2D-DWT), HWT relies on the use of two independent factors $a_1 = 2^{j_1}$ and $a_2 = 2^{j_2}$ along directions x_1 and x_2 respectively. The Hyperbolic Wavelet coefficients of imaged paper i , denoted as $T_i((a_1, a_2), (k_1, k_2))$ are theoretically defined as:

$$T_i((a_1, a_2), (k_1, k_2)) = \langle i(x_1, x_2), \frac{1}{\sqrt{a_1 a_2}} \psi\left(\frac{x_1 - k_1}{a_1}, \frac{x_2 - k_2}{a_2}\right) \rangle. \quad (2)$$

From these HWT coefficients, structure functions, consisting of space averages at given scales a_1, a_2 , are defined as:

$$S_i((a_1, a_2), q) = \frac{1}{n_a} \sum_{\underline{k}} |T_i((a_1, a_2), (k_1, k_2))|^q, \quad (3)$$

where n_a stands for the number of $T_i((a_1, a_2), (k_1, k_2))$ actually computed and not degraded by image border effects.

To measure proximity between two images i and j , a cepstral distance between their structure functions $S_i((a_1, a_2), q)$ and $S_j((a_1, a_2), q)$ is computed. It consists of a classical L^p norm computed on log-transformed normalized structure functions:

$$d(i, j) = \left(\sum_a | \bar{S}_i(a, q) - \bar{S}_j(a, q) |^p \right)^{\frac{1}{p}} \quad \text{with} \quad (4)$$

$$\bar{S}_i(a, q) = \ln \frac{S_i(a, q)}{\sum_{a'} S_i(a', q)}. \quad (5)$$

4. Pseudo-area-scale analysis (WPI)

Area-scale analysis is a technique which has been applied to various problems in surface metrology.[15] Much as the measured length of a coastline depends on the scale of observation and therefore the resolvability of small features, the measured area of a surface is also a function of the scale of observation. The area-scale approach uses fractal analysis to decompose a surface into a patchwork of triangles of a given size. As the size of the triangles is increased, smaller surface features become less resolvable and the ‘relative area’ of the surface decreases. The topological similarity of two surfaces is computed by comparing relative areas

at various scales. The technique has traditionally been employed on topographic data sets containing height information over a surface. Though lacking a direct measure, area-scale analysis can be applied to the photomicrographs using light intensity as a proxy for height.

The proposed approach proceeds in three steps: (1) preprocessing, (2) feature extraction, and (3) classification. The preprocessing step extracts a square $N \times N$ region from the center of the image (where N was chosen to be 1024), and normalizes the intensity of the resulting extracted image. The $N \times N$ grid of equally spaced points (representing pixel locations) is decomposed into a patchwork of

$$2\left(\frac{N-1}{s}\right)^2 \quad (6)$$

isosceles right triangles where s is a scale parameter representing the length of two legs of each triangle. The pixel values at each of the triangle vertices are then taken as the ‘pseudo-height’ of each of the vertices. The area of each triangle in 3-D space is then computed and the areas of all triangular regions are summed, resulting in the total relative area A_s at the chosen scale s . To conduct feature extraction, the relative area for an image is computed over a range of scale values; in this study, 8 scale values were used ranging from 1 pixel to 34 pixels, which correspond to lengths of $6.51 \mu\text{m}$ to 0.221 mm , respectively. Finally, to classify and compare the similarity of two images i and j , a χ^2 distance measure $d(i, j)$ is computed via

$$d(i, j) = \sum_{s \in S} \frac{(A_s^{(i)} - A_s^{(j)})^2}{A_s^{(i)} + A_s^{(j)}} \quad (7)$$

where $A_s^{(i)}$ is the relative area of image i at scale s and S is the set of chosen scale values. Small values of $d(i, j)$ indicate high similarity between images i and j , while large values indicate low similarity.

Results as Affinity Maps

From the metadata and each of the teams’ automatic classifiers, the degree of similarity (affinity) was tabulated for each possible pairing of images in the 120-sample dataset. These scores were then converted to a grey-scale with the darkest intensities indicating the greatest affinity and the lightest the least affinity. To visualize these values a table containing 120 rows and 120 columns was created, one row and column for each sample in the data set. Each of the resulting 14,400 cells in the table was shaded according to the similarity of compared samples with black describing an exact match, white a total mismatch and gray-scale values in between describing a range of better or worse similarities. For example, the top diagram in Figure 3, shows predicted similarities within the sample group suggested by the metadata listed in the Appendix, including manufacturer, texture, brand, and date (these affinities were prepared solely on the metadata and not on direct examination of the surfaces). As expected, the six dark blocks starting in the upper left and continuing down along the diagonal, show a high degree of affinity (dark gray and black) as these blocks depict the groups derived from the same sheet or package. Lesser degrees of similarity are scattered throughout the figure with the 30 samples selected to show diversity (poorer levels of similarity) falling in the lower right quadrant and along the right side and bottom edge.

Gray-scale affinity maps produced to display the results from each of the four teams are also shown in Figure 3. The principal similarity among the five affinity maps in Figure 3 are the six dark squares

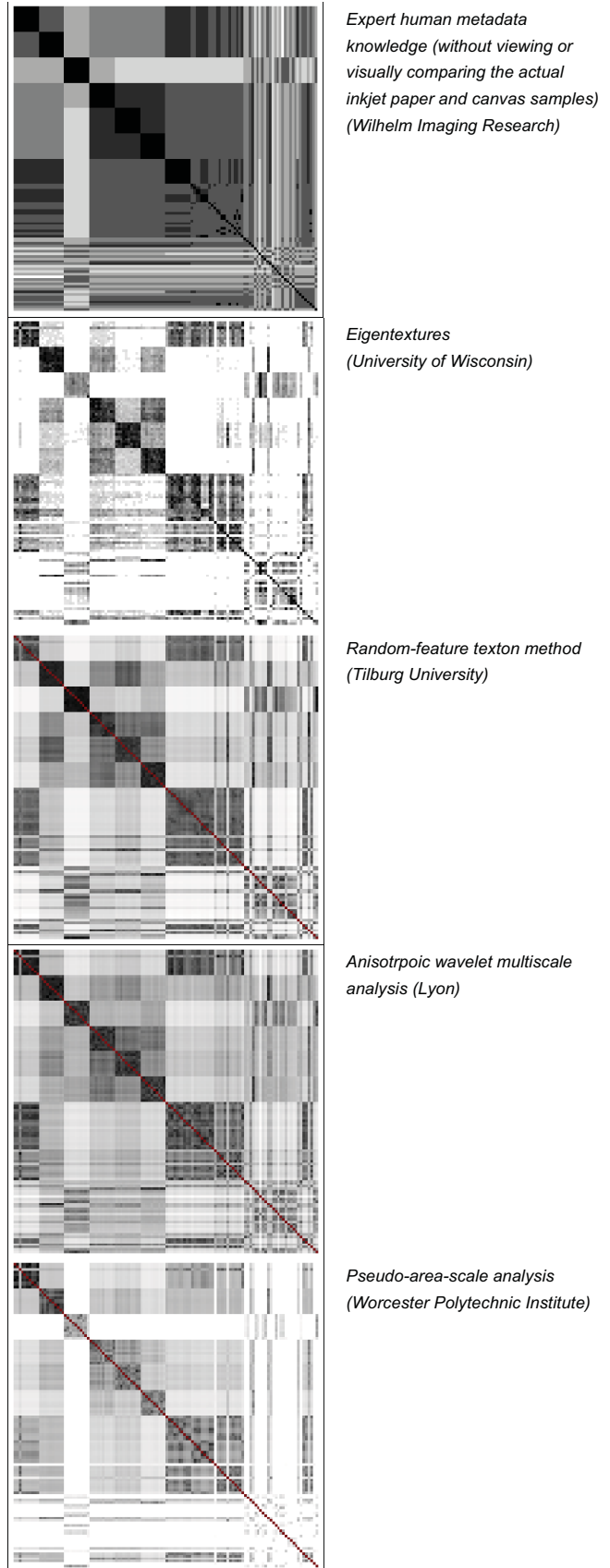


Figure 3. Affinity maps of Affinities (dark: strong, light: weak)

along the upper left to lower right diagonal. Given the construction of the dataset, these blocks should be dark due to the similarity between the samples in these groups. The light stripes in the right and bottom quarters of the affinity maps, due to some relatively matchless textures among samples 91-120, are also shared by all five affinity maps.

While small local differences among the five maps indicate that work remains to find an ideal automated scheme, striking fundamental similarities between the metadata-based affinity map and the four produced by automated schemes validate raking light photomicrographs as having sufficient texture information to support the automated classification of inkjet paper.

Observations

As shown in Figure 3, there is a relatively high level of agreement between the affinity pairings prepared by the classification algorithms and those derived from metadata and subject-matter expertise. As discussed in the previous section, the principal correspondence among the five affinity maps is the six dark squares along the diagonal running from upper left to lower right. Given the construction of the dataset, the samples in these blocks are very similar and these texture affinities were recognized both by a subjective metadata sort and by the four automated solutions. In addition, both “human” and automated solutions are sensitive to the increased levels of diversity within samples 61-90 that track a manufacturer’s surface over time.

These findings are reinforced by Figure 4, which shows a normalization of the distances between each texture pairing within the tested groups. The shape of the curves are remarkably consistent with the automated solutions and the human metadata-based classification detecting very similar degrees of affinity across the groups. The chart confirms there is no measurable difference between texture images made from the same sheet of paper as compared to images made from different sheets from the same manufacturer package. Further, textures produced to same manufacturing standard over time show fair to good levels of similarity (blocks 7, 8 & 9). These results, though not a surprise given high levels of manufacturing regularity, are important for the possible development of future systems that rely on indices of known “exemplar” textures to identify unknowns.

Compared with the 120 silver gelatin surfaces assessed in the previous study, the inkjet materials were found to be more diverse. Smooth inkjet papers were observed to be significantly more uniform as compared to smooth (non-ferrotyped) silver gelatin papers. On the other end of the scale, the rougher inkjet canvas finishes showed significantly more dimensionality than any of the tested silver gelatin surfaces. Another difference is the relative lack of stronger affinities within diagonal blocks 7, 8 & 9 in Figure 3. Silver gelatin papers showed higher levels of consistency in these groups of papers identified as having the same manufacturer specifications over a period of time. Aside from these differences, the results for both the inkjet and silver gelatin surfaces are highly comparable especially for the generally good alignment between the human expert’s affinity expectations and the measured affinities generated by the teams.

Conclusions and Next Steps

This project opens a path toward a machine vision system that provides meaningful results for the study of inkjet prints. To have meaning, an automated classification system cannot produce results simply based on an internal, self-referential “sameness/difference” parameter but instead must render results that are relevant to trained practitioners, such as media manufacturers, conservators and curators. For example, the photomicrographs

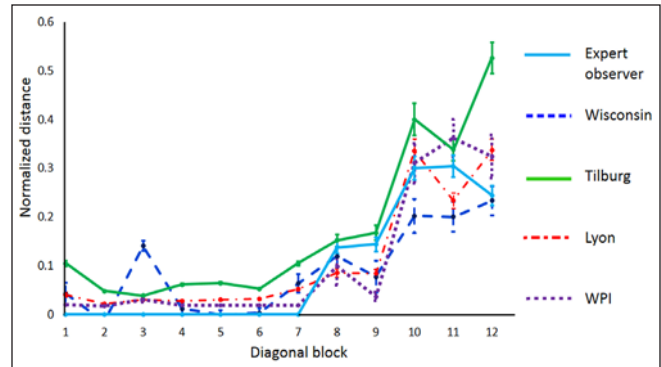


Figure 4. Normalized image pair distances for the dataset of texture images (Diagonal blocks 1-3 same sheet, 4-6 same package, 7-9 same manufacturing standard and, 10-12 diverse samples).

made from ten spots on the same sheet of paper, though totally different images, need to be recognized as the “same.” Likewise the two other similarity groups made from different sheets from the same manufacturer’s package and from papers manufactured to the same standard must be recognized as related.

A useful system needs to reliably cluster these groups together while at the same time be discriminating enough to set these groups apart from others made to different manufacturer specifications. Using different techniques, each of the four teams met this standard. The fundamental outcome of this experiment is the intuitive “human / expert observer” conception of a classification system based on sameness / difference can be replicated through imaging and signal processing techniques.

The techniques described in this work could engender new modes of scholarship based on the discovery of materials-based affinities. Work at the Museum of Modern Art is underway to determine how these techniques might meaningfully be applied to silver gelatin prints in its Thomas Walther Collection. Moving forward, reference libraries of surface textures, containing papers grouped by photographer or paper manufacturer can be assembled and used as a basis of comparison.

This work has already begun through the assembly of large photographic and inkjet paper and canvas reference collections categorized by manufacturer, brand, surface finish, and date as well as for individual photographers and artists.

When used together with image and dot structure photomicrographs, spectral reflectance data in the UV, visible, and IR regions, gloss and DOI measurements, surface characterization is an important tool in the identification, dating, and authentication of inkjet prints. With standardized imaging techniques and a networked infrastructure, conservators and others could query such texture libraries to detect similar papers held by other collections, potentially characterizing and identifying works in their collection as well as revealing relationships within an photographer’s body of work and between photographers. Having shown promise for both silver gelatin papers and inkjet, these methodologies are being applied to other media, including the platinum papers of F. Holland Day (1864-1933). A website, www.PaperTextureID.org, has been created to distribute the dataset of silver gelatin and inkjet textures used as the basis for this study. The availability of these image sets should encourage and assist other image processing and programming teams to develop their own automated classification and sorting schemes.

Appendix: Inkjet Paper and Canvas Samples Used in the Dataset

The number is the sequential numbering system suggested by the teams following image processing. The papers are further identified by manufacturer, brand, manufacturer location and date (date generally refers to the acquisition date of papers). Other descriptors, such as surface finish designations, are taken directly from the manufacturer packaging. All samples were drawn from the *Wilhelm Analog and Digital Color Print Materials Reference Collection*.

10 samples from the same sheet (X 3 sheets)

- 1-10. Canon Platinum Pro, Smooth, Glossy: Japan, Purchased 4/2012
- 11-20. Ilford Gallerie Gold Fibre Silk, Smooth, Glossy: Germany, ~ 2009
- 21-30. Hahnemuhle Fine Art William Turner, Textured, Matte: Germany, ~2009

10 samples from the same package (X 3 packages)

- 31-40. Epson Premium Luster Photo Paper (roll), Smooth, Semi-Glossy: Japan, Purchased 8/2002
- 41-50. Epson Ultra Premium Photo Paper Luster (Formerly called Epson Premium Photo Paper Luster), Smooth, Semi-Glossy: Japan, Purchased 7/2011
- 51-60. Epson Sample Roll Premium Luster Photo Paper, Smooth, Semi-Glossy: Japan, ~ 2001

10 samples from the same (or similar) manufacturing standard (X 3 sets)

- 61. HP Premium Plus Photo Paper, High gloss, Smooth, Glossy: United States, 2006
- 62. HP Premium Plus, Glossy Photo Paper, Smooth, Glossy: Switzerland, 2002
- 63. HP Premium Plus Photo Paper, glossy, Smooth, Glossy: UK, 2001
- 64. HP Premium Plus Photo Paper, High gloss, Smooth, Glossy: United States, 2005
- 65. HP Premium Plus High Gloss Photo Paper, Smooth, Glossy: Switzerland, 2004
- 66. HP Premium Plus Photo Paper, High gloss, Smooth, Glossy: Switzerland, 2005
- 67. HP Premium Plus Photo Paper, High gloss, Smooth, Glossy: Switzerland, 2006
- 68. HP Premium Plus Photo Paper, High gloss, Smooth, Glossy: United States, 2007
- 69. HP Premium Plus Photo Paper, glossy, Smooth, Glossy: Switzerland, 2002
- 70. HP Premium Plus Photo Paper, High gloss, Smooth, Glossy: Switzerland, 2007
- 71. Epson Photo Quality Glossy Film, Smooth, Glossy: Japan, ~ 1996
- 72. Epson Photo Paper Glossy, Smooth, Glossy: Germany, Purchased 02/2008
- 73. Epson Premium Photo Paper Glossy (Formerly Premium Glossy Photo Paper), Smooth, Glossy: Japan, Purchased 03/29/2008
- 74. Epson Premium Photo Paper Glossy (Formerly Premium Glossy Photo Paper), Smooth, Glossy: Japan, Purchased 03/08/2008
- 75. Epson Ultra Premium Glossy Photo Paper, Smooth, Glossy: Japan, Purchased 03/2007
- 76. Epson Ultra Premium Photo Paper Glossy (Formerly Ultra Premium Glossy Photo Paper), Smooth, Glossy: Japan, Purchased 02/2008
- 77. Epson Ultra Premium Glossy Photo Paper, Smooth, Glossy: Japan, Purchased 02/2007
- 78. Epson Photo Paper Glossy (Formerly Glossy Photo Paper), Smooth, Glossy: Germany, Purchased 02/2007
- 79. Epson Premium Glossy Photo Paper, Smooth, Glossy: Japan, Purchased 06/2004
- 81. Kodak Ultima Picture Paper, High Gloss, Smooth, Glossy: Canada, Purchased 12/2003
- 82. Kodak Ultra Premium Photo Paper, High Gloss, Smooth, Glossy: Germany, Purchased 11/2011

- 83. Kodak Premium Photo Paper, Gloss, Smooth, Glossy: Germany, Purchased 06/2011
- 84. Kodak Premium Picture Paper, High Gloss, Smooth, Glossy: Canada, Purchased 12/2003
- 85. Kodak Photo Paper, Gloss, Smooth, Glossy: Germany, Purchased 03/2009
- 86. Kodak Ultima Picture Paper, High Gloss, Smooth, Glossy: Canada, ~ 2002
- 87. Kodak Professional Inkjet Photo Paper, Smooth, Glossy: USA, Purchased 7/2004
- 88. Kodak Premium Picture Paper, High Gloss, Smooth, Glossy: Canada, Purchased 04/2003
- 89. Kodak Ultima Picture Paper, Ultra Glossy, Smooth, Glossy: Canada/UK, Purchased 03/2004
- 90. Kodak Premium Photo Paper, Gloss, Smooth, Glossy: Germany/USA, Purchased 03/2007

30 samples showing diversity

- 91. Epson Ultra Premium Glossy Photo Paper, Smooth, Glossy: Japan, ~ 2005
- 92. Epson Ultra Premium Presentation Paper, Smooth, Matte: Japan, Purchased 4/2007
- 93. Canon Fine Art Paper Premium Matte, Smooth, Matte: Japan, ~ 2006
- 94. Canon Photo Paper Pro II, Smooth, Glossy: Japan, Purchased 12/2008
- 95. Epson Sample Roll Premium Luster Photo Paper, Smooth, Semi-Glossy: Japan, ~ 2001
- 96. Canson BFK Rives, Textured, Matte: France, Purchased 4/2008
- 97. Canson Rag Photographique, Smooth, Matte: France, Purchased 4/2008
- 98. Canson Museum Canvas Water Resistant Matte, Canvas/Textured, Matte: France, Purchased 4/2008
- 99. Canson Velin Museum Rag, Smooth, Matte: France, Purchased 4/2008
- 100. Canson Arches Aquarelle Rag, Textured, Matte: France, Purchased 4/2008
- 101. Ilford Gallerie Gold Fibre Silk, Smooth, Glossy: Germany, ~ 2009
- 102. Epson Exhibition Fibre Paper, Smooth, Soft-Gloss: Japan, Purchased 11/1/2007
- 103. Canson Artist Canvas Water Resistant Matte, Canvas, Matte: France, Purchased 04/2008
- 104. Epson Water Color Paper-Radiant White, Textured, Matte: Japan, ~ 2000
- 105. Canson Artist Canvas Professional Gloss, Canvas, Glossy: France, Purchased 04/2008
- 106. Canson Mi-Teintes, Honeycomb, Matte: France, Purchased 04/2008
- 107. Canson Edition Etching Rag, Smooth, Matte: France, Purchased 04/2008
- 108. Canson Montval-Torchon, Textured, Matte: France, Purchased 03/2008
- 109. Epson Cold Press Bright, Cold-Press Textured, Matte: Italy, Purchased 08/2010
- 110. Epson Hot Press Bright, Hot-Press Smooth, Matte: Italy, Purchased 03/2011
- 111. Epson Cold Press Natural, Cold-Press Textured, Matte: Italy, Purchased 8/2010
- 112. Epson Hot Press Natural, Hot-Press Smooth, Matte: Italy, Purchased 3/2011
- 113. Canon Photo Paper Pro (PR-101), Smooth, Glossy: Japan, ~ 2006
- 114. Canon Matte Photo Paper (MP-101), Smooth, Matte: Japan, ~ 2007
- 115. Ilford Galerie Smooth Gloss, Smooth, Glossy: Switzerland, ~ 2009
- 116. HP Premium Plus Photo Paper, High Gloss, Smooth, Glossy: Switzerland, ~ 2005
- 117. Epson ColorLife Photo Paper Semi Gloss, Smooth, Semi-Glossy: Switzerland, Purchased 2/2004
- 118. Kodak Ultima Picture Paper, Satin, Smooth, Glossy: Canada, ~ 2000
- 119. Epson Premier Art Matte Scrapbook Photo Paper, Smooth, Matte: Japan, ~ 2003
- 120. Hahnemuhle Fine Art William Turner, Textured, Matte: Germany, ~ 2009

References

- [1] P. Messier, "Les Emulsion Industrielles," in *Le Vocabulaire Technique de la Photographie*, ed. A. Cartier-Bresson. (Les Editions Marval. Paris, 454–456 (2008).
- [2] Eastman Kodak Company. *Surface Characteristics of Kodak Photographic Papers*, Eastman Kodak Company, Rochester, NY (ca. 1935).
- [3] P. Messier, M. Messier, and C. Parker. Query and retrieval systems for a texture library of photographic papers. *Proc. of the International Conference on Surface Metrology*, I–10 (2009).
- [4] C. Parker and P. Messier. Automating Art Print Authentication Using Metric Learning, *Proceedings of the Twenty-First Innovative Applications of Artificial Intelligence Conference*, Association for the Advancement of Artificial Intelligence: 122–127 (2009).
- [5] R. Johnson and P. Messier. Pursuing Automated Classification of Historic Photographic Papers from Raking Light Photomicrographs. Submitted to the *Journal of the American Institute for Conservation*, draft: http://papertextureid.org/pdf/JAIC-HPPC_submitted_5_24_13.pdf (2013, accessed 07/17/13).
- [6] H. Wilhelm, C. Brower, K. Armah, and B. Stahl. The Wilhelm Analog and Digital Color Print Materials Reference Collection, <http://www.wilhelm-research.com> (2013, accessed 07/17/13).
- [7] R. Haralick, R. M. Statistical and structural approaches to texture. *Proc. of the IEEE*, 67(5):786–804 (1979).
- [8] R. Gonzalez and R. Woods. *Digital Image Processing*, Third edition. Prentice Hall, Upper Saddle River, NJ (2008).
- [9] T. K. Moon and W. C. Stirling. *Mathematical Methods and Algorithms for Signal Processing*. Prentice Hall, Upper Saddle River, NJ, 3.4:138–141 and 7:369–395 (2000).
- [10] L. Liu and P. W. Fieguth. Texture classification from random features. *IEEE Transactions on Pattern Analysis and Machine Intelligence*, 34(3):574–86 (2012).
- [11] M. Varma and A. Zisserman. A Statistical Approach to Material Classification Using Image Patch Exemplars. *IEEE Transactions on Pattern Analysis and Machine Intelligence*. 31(11): 2032–2047 (2009).
- [12] R. DeVore, S. Konyagin, and V. Temlyakov. Hyperbolic wavelet approximation. *Constructive Approximation*. 14:1–26 (1998).
- [13] S. Roux, M. Clausel, B. Vedel, S. Jaffard, and P. Abry. Self-Similar Anisotropic Texture Analysis: The Hyperbolic Wavelet Transform Contribution. <http://arxiv.org/abs/1305.4384v1> (accessed 07/17/13).
- [14] S. Mallat. *A Wavelet Tour of Signal Processing*, Third Edition: The Sparse Way. Academic Press, San Diego, CA (2009).
- [15] C. Brown, P. Charles, W. Johnsen, and S. Chestera. Fractal analysis of topographic data by the Patchwork method. *Wear*, 161, 61–67 (1993).

Presenter Biographies

Paul Messier is a conservator of photographs working in Boston Massachusetts, USA. Founded in 1994, his studio provides conservation services for private and institutional clients throughout the world. The heart of this practice is unique knowledge and ongoing research into photographic papers. Messier is the corresponding author. Address: 103 Brooks Street, Boston, MA 02135. Email: pm@paulmessier.com.

Henry Wilhelm is co-founder and director of research at Wilhelm Imaging Research, Inc. Through its website, www.wilhelm-research.com, the company publishes print permanence data for desktop and large-format inkjet printers, silver-halide color papers, and digital presses. Wilhelm Imaging Research also provides consulting services to museums, archives, and commercial collections on sub-zero cold storage for the very long-term preservation of still photographs and motion pictures. Address:

Wilhelm Imaging Research, Inc., 713 State Street, P.O. Box 775, Grinnell, Iowa 50112 USA. Email: hwillhelm@aol.com.

C. Richard Johnson, Jr. received a PhD in Electrical Engineering and a PhD minor in Art History Stanford University. He is currently the Geoffrey S. M. Hedrick Senior Professor of Engineering and a Stephen H. Weiss Presidential Fellow at Cornell University, Ithaca, NY. His current research interest is computational art history. Address: School of Electrical and Computer Engineering, 390 Rhodes Hall, Cornell University, Ithaca, NY 14853 USA. Email: johnson@ece.cornell.edu.

Acknowledgements

The authors are deeply grateful for the contributions of Christopher Brown and Anh Hoang Do of the Worcester Polytechnic Institute and Philip Klausmeyer of the Worcester Art Museum. We also wish to acknowledge the vital assistance of James Coddington, Lee Ann Daffner and Hanako Murata of the Museum of Modern Art, as well as Sally Wood, Mark Messier and Andrew Messier.



William Sethares examining raking light photomicrographs of paper surface textures at a meeting at the Museum of Modern Art in New York in January 2013. Sethares, who teaches at the University of Wisconsin at Madison, is one of the signal processing experts who contributed to this study. The meeting was hosted by Jim Coddington, Lee Ann Daffner, and Hanako Murata, conservators at MoMA.



A meeting held at the San Francisco Museum of Modern Art in July 2012. Richard Johnson (left) who organized this project with Paul Messier, is a professor at Cornell University. The meeting was hosted by SFMoMA conservators Jill Sterret and Theresa Andrews. (Photos by Henry Wilhelm)

Automated Surface Texture Classification of Inkjet and Photographic Media

Paul Messier; Paul Messier LLC, Boston, MA USA; Richard Johnson; Cornell University, Ithaca, NY USA; Henry Wilhelm; Wilhelm Imaging Research, Inc., Grinnell, Iowa USA; William A. Sethares; University of Wisconsin, Madison, WI, USA; Andrew G. Klein; Worcester Polytechnic Institute, Worcester, MA USA; Patrice Abry; Ecole Normale Supérieure de Lyon, Centre National de la Recherche Scientifique, Lyon FR; Stéphane Jaffard; University of Paris, Paris FR; Herwig Wendt, Institute de Recherche en Informatique de Toulouse, Centre National de la Recherche Scientifique; Toulouse, FR; Stéphane Roux, Ecole Normale Supérieure de Lyon, Lyon FR; Nelly Pustelnik, Ecole Normale Supérieure de Lyon, Centre National de la Recherche Scientifique, Lyon FR; Nanne van Noord, Laurens van der Maaten, and Eric Postma; Tilburg University, Tilburg, NL

Paper presented by Paul Messier and Henry Wilhelm on September 30, 2013

Paper (monochrome, with no color) published on pages 85–91 in:

Technical Program and Proceedings: NIP29: The 29th International Conference on Digital Printing Technologies

IS&T: The Society for Imaging Science and Technology
and ISJ: The Imaging Society of Japan

September 29 – October 3, 2013
Westin Seattle Hotel
Seattle, Washington U.S.A.

ISBN: 978-0-89208-306-0

©2013 The Society for Imaging Science and Technology

Published by:
IS&T: The Society for Imaging Science and Technology
7003 Kilworth Lane
Springfield, Virginia 22151 U.S.A.
Phone: 703-642-9090; Fax: 703-642-9094
www.imaging.org (e-mail: info@imaging.org)